energies

MDPI

Article

Numerical Investigation of the Impact of H_2 Enrichment on Lean Biogas/Air Flames: An Analytical Modelling Approach

Filipe M. Quintino * and Edgar C. Fernandes

Center IN+, Instituto Superior Técnico, University of Lisbon, 1049-001 Lisbon, Portugal; edgar.fernandes@tecnico.ulisboa.pt

* Correspondence: filipe.marques.quintino@tecnico.ulisboa.pt

Abstract: The transition from natural gas to renewable gases such as biogas and hydrogen creates an interchangeability challenge. The laminar flame speed S_L is a critical parameter in appliance design as it is a unique characteristic of the flame mixture. It is thus essential to evaluate the impact of renewable gases on S_L. In this work, 1D simulations were conducted in Cantera with the USC-Mech 2.0 kinetic mechanism. The S_L of three base biogas blends (BG100, BG90 and BG80) was computed for H_2 enrichment up to 50% in volume, equivalence ratio $0.8 \leq \phi \leq 1.0$, $p = 1$ atm and $T_u = 298$ K. It was found that the effect of H_2 enrichment is higher for base blends with higher CO_2 content as the thermal-diffusive and dilution effects of carbon dioxide are mitigated by hydrogen. The introduction of H_2 also increases the H radical pool, which is linked with the increase in S_L. A new correlation to model the impact of H_2 enrichment, $S_L(x_{H_2}) = \left(\zeta(\phi)/S'_L(x_{CO_2})\right)x_{H_2}e^{x_{H_2}} + S'_L(x_{CO_2})$, is proposed, which exhibits good agreement with the literature data and simulations. This equation can be directly used to estimate S_L without the need for a priori adaptations of fit parameters as the contributions of CO_2 and H_2 are isolated in independent variables.

Keywords: biogas; hydrogen; laminar flame speed; premixed combustion; correlation

Citation: Quintino, F.M.; Fernandes, E.C. Numerical Investigation of the Impact of H_2 Enrichment on Lean Biogas/Air Flames: An Analytical Modelling Approach. *Energies* **2021**, *14*, 369. https://doi.org/10.3390/en14020369

Received: 16 December 2020
Accepted: 6 January 2021
Published: 11 January 2021

1. Introduction

Natural gas is a widely used fuel in applications ranging from heating and electricity generation to cooking and vehicle fuel [1]. However, the increasingly ambitious greenhouse gas (GHG) emission reduction targets, set by governments and institutions, means that it will likely be phased out in the future. As many of its current applications are not easily adaptable to consume electricity, renewable gases will be required. Recent developments in technology and public policy have opened a pathway where hydrogen and biogas are the likely candidates to replace natural gas [2–5].

Biogas is a biofuel obtained from the anaerobic digestion of organic matter. Its main components are CH_4 and CO_2, and it is often upgraded to biomethane by removing the excess carbon dioxide [6]. As biogas exhibits a similar composition to natural gas, with methane occupying the largest volume share in both, it has been widely used in its place in the past. In Denmark, for example, more than 50% of the biogas produced in the country is upgraded and injected in the national gas grid [7]. However, the limited feedstock for biogas production in most countries indicates that it cannot solely meet the gas demand. Therefore, green hydrogen has been pointed out as a more scalable alternative. It can be produced through electrolysis, requiring only a source of water and electricity [8]. By producing hydrogen through electrolysis, it is possible to couple the gas and electricity sectors, taking advantage of off-peak hours electricity production. However, replacing natural gas with hydrogen raises additional concerns as the two fuels have significantly different properties. The introduction of hydrogen and biogas in the energy sector is expected to be gradual by incorporating larger shares of renewable gases as time goes on. Several countries have already established targets for the use of renewable gases,

particularly hydrogen, at least until 2030. Based on national strategies and roadmaps, a summary of these for selected countries is provided in Table 1:

Table 1. Hydrogen related targets in selected countries for 2030. Data collected from national hydrogen roadmaps.

Country	Electrolyser Capacity (GW)	Hydrogen Refuelling Stations	Hydrogen Share in Gas Networks (%)
France	6.5	400–1000	-
Germany	5	-	-
Japan	-	900	-
Netherlands	3–4	-	-
New Zealand	-	-	20
Portugal	2–2.5	50–100	10–15
South Korea	-	310–1200	-
Spain	4	100–150	-

A major challenge in the transition from natural gas to renewable gases in the gas system is the interchangeability in end-use equipment [9]. These devices are often tailored for a specific fuel composition, thus having a unknown performance when this changes. Therefore, it is crucial to effectively determine the impact of different levels of renewable gas incorporation in current gas systems in a fast and accessible way. Significant impacts on reaction chemistry are expected due to high concentrations of CO_2 and H_2 in the gas composition resulting from hydrogen and biogas admixture. The sub-mechanism of the water-gas shift (WGS) reaction ($CO + H_2O \rightleftharpoons CO_2 + H_2$) is of particular importance in hydrogen applications. This reaction appears through the combination of the CO oxidation and a radical shuffle reaction [10]:

$$CO + OH \rightleftharpoons CO_2 + H \quad (1)$$

$$H_2O + H \rightleftharpoons OH + H_2 \quad (2)$$

Changes in reaction kinetics will ultimately have an impact on the laminar flame speed S_L, a critical parameter in appliance design. This unique characteristic of a premixed combustion mixture depends on the reaction rate, thermal diffusivity and temperature in the flame region [11]. Consequently, a precise determination of S_L is of the utmost importance in design and equipment performance.

The estimation of S_L is often time-consuming. It can be experimentally measured, which often makes the process expensive, or obtained using numerical models. However, these methods require extensive and detailed kinetics mechanisms, which increase the computational cost [12]. As a result, there has been an effort to develop empirical and analytical relations to estimate S_L for varied blends and conditions [13]. Several authors have focused on the impact of diluents in S_L to address a challenge posed by exhaust gas recirculation (EGR) systems. Metgalchi and Keck [14], in 1982, established a "power-law" relation, which has been widely adopted [15,16]:

$$S_L = S_{L,ref} \left(\frac{p}{p_{ref}} \right)^{\sigma} \left(\frac{T_u}{T_{u,ref}} \right)^{\gamma} (1 - 2.1 y_{dil}) \quad (3)$$

where $S_{L,ref}$ is the laminar flame speed at pressure $p = p_{ref}$ and unburned gas temperature $T_u = T_{u,ref}$ for a determined equivalence ratio ϕ. $\sigma = \sigma(\phi)$ and $\gamma = \gamma(\phi)$ are fit parameters and y_{dil} the mass fraction of diluents in the premixed combustion mixture. The formulation of Equation (3) was based on experimental data obtained for propane, methanol, isooctane and indolene tested in a constant volume bomb experiment. The diluent simulated an EGR gas mixture (85%N_2/15%CO_2). Since then, other authors explored alternative formulations. Han et al. [17] tested CH_4/EGR mixtures, where EGR=81.5%N_2/18.5%CO_2, obtaining the

following correlation from empirical data: $S_{L,ref} = 229.7D^2 - 157.6D + 35.26$, where D is the volume fraction of EGR in the mixture. Elia et al. [18] proposed the following expression for a diluent mixture composed of 86%N_2/14%CO_2: $S_L/S_{L,ref} = 1 - a_1D + a_2D^2 + a_3D^3$, where D is the diluent volume fraction (in %) and a_i are model parameters.

Biogas composition is highly variable depending on the substrate used in production, as well as on the anaerobic digestion process, which, in turn, is affected by several technical aspects. As a result, the weight of CH_4 and CO_2 in the blend composition varies significantly, thus changing the laminar flame speed. Hydrogen can be used to compensate the changes in S_L caused by increases in CO_2 content to attain a relatively steady value of S_L that ensures adequate equipment performance and safety. However, to do this, an accurate estimation of the H_2 enrichment impact on the laminar flame speed is necessary, to ensure that changes in S_L are not over- or under-compensated by the hydrogen admixture. In 2011, based on the original formulation of Metgalchi and Keck (Equation (3)), Bougrine et al. [19] proposed a new correlation to model S_L in CH_4/H_2 flames. To this end, the authors performed one-dimensional simulations and collected literature data across a wide set of conditions. Even though the resulting model exhibited good agreement with premix simulations, it required the determination of 40 fit parameters, making its use not expeditious. Furthermore, biogas was not directly addressed in this research.

Recently, Quintino and Fernandes [20] explored the possibility of using an analytical correlation to model the impact of CO_2 content on the S_L of biogas/air lean flames. Based on the formulation of Equation (3), a new expression was obtained, exhibiting good results for a mass fraction of CO_2 ($y_{CO_2,dil}$) in the flame up to 0.38. The model parameters were estimated using data from one-dimensional numerical simulations. Furthermore, the expression performance was also evaluated with available literature results. The final model took the form of Equation (4):

$$S_L = S_{L,ref}\left(\frac{p}{p_{ref}}\right)^{\sigma}\left(\frac{T_u}{T_{u,ref}}\right)^{\gamma}\left(1 + \alpha y_{dil} + \beta y_{dil}^2\right) \quad (4)$$

where p and T_u are the pressure and temperature of the unburned mixture, respectively, $p_{ref} = 1$ atm and $T_{u,ref} = 298$ K, $S_{L,ref} = S_{L,ref}(\phi)$ is the laminar flame speed at reference conditions and $y_{dil} = 0$ and $\alpha = \alpha(\phi)$, $\beta = \beta(\phi)$, $\sigma = \sigma(\phi)$ and $\gamma = \gamma(\phi)$ are model parameters. More details on the model can be found in the original paper [20]. This correlation failed to incorporate the possibility of hydrogen enrichment, making it possible to assess the drop in S_L for a determined CO_2 content, but not to estimate the H_2 admixture necessary to compensate such a drop.

This work aims to study the impact of H_2 enrichment on the laminar flame speed of lean biogas/air flames and to develop an analytical correlation to model S_L, extending the application range of Equation (4). To that end, one-dimensional simulations in Cantera software are conducted for three base biogas blends (BG100, BG90 and BG80), with the equivalence ratio between 0.8 and 1.0 and hydrogen content in the fuel mixture up to 50% in volume. The impacts of thermal-diffusive, dilution and chemical effects of CO_2 and H_2 on S_L at $p = 1$ atm and $T_u = 298$ K are analysed. A correlation is proposed and validated with simulations and literature data.

2. Methods

2.1. Modelling

Simulations were conducted using the CANTERA toolkit [21] in the Python (Version 3.7) programming language (Python Software Foundation, http://www.python.org/). The laminar flame speed S_L for each blend and condition were obtained with a one-dimensional freely propagating flame routine (FPF). Steady-state and uniform inlet conditions were assumed in every run. The computational domain was defined with a sufficient size to ensure negligible heat and mass diffusion through the boundary. Inlet pressure and temperature were set to $p = 1$ atm and $T_u = 298$ K, respectively.

The 1D FPF routine was fed with the USC Mech 2.0 kinetics mechanism [22], published in 2007 by the Combustion Kinetics Laboratory of the University of Southern California. It comprises 111 chemical species and 784 reactions and is tailored for the combustion of $H_2/CO/C_1$-C_4 based blends. This mechanism has overall presented good results with $CH_4/CO_2/H_2$ fuels in engine simulations [23] and in the estimation of laminar premixed combustion characteristics [24,25].

Three base biogas blends were adopted for the conducted simulations: BG100, BG90 and BG80. Under the notation BGXX, XX indicates the volume content (v/v %) of CH_4 in the blend, while the remainder is assumed to be CO_2. Previous research has shown that the presence of small quantities of other ballast components in biogas have little impact on S_L values [20], indicating that modelling of biogas as a CH_4/CO_2 mixture is a valid assumption for this work. The impact of hydrogen enrichment for each biogas blend was also evaluated. H_2 content by volume in the fuel (x_{H_2}) varied between 0% and 50%, with 1 p.p.steps. It was calculated as:

$$x_{H_2} = \frac{n_{H_2}}{n_{CH_4} + n_{CO_2} + n_{H_2}} \tag{5}$$

where x_{H_2} is the hydrogen content in the fuel blend and n_i[mol] the amount of species i. The combustion reaction equivalence ratio ϕ varied in the interval $0.8 \leq \phi \leq 1.0$, with 0.05 steps. Air was assumed to be only O_2 and N_2 in a 21/79% proportion. Every base biogas blend was simulated at every ϕ and x_{H_2} detailed above.

2.2. Correlation

As stated before, this work intends to develop an analytical correlation to model the impact of H_2 enrichment on the S_L of lean biogas/air flames. Based on the model outputs, a correlation was obtained using a best fit routine. To do so, several formulations based on the exponential behaviour were tested. This was performed using the `curve-fit()` function of the SciPy (Version 1.5.4) module in Python. The routine tests a function formulation and determines the parameters that provide the best fit. Simplicity was prioritized in the choice of the mathematical formulation. It was ensured that the obtained correlation attained an $R^2 \geq 0.99$ for every base blend and ϕ. Furthermore, it was also guaranteed that correlation parameters were independent of CO_2 content (x_{CO_2}) in the base biogas blend except for an intermediate flame speed S'_L, which already accounts for the carbon dioxide contribution. The expressions tested assumed the following formulation:

$$S_L = S_L(x_{H_2}, \phi, S'_L) \tag{6}$$

where S_L[m/s] is the laminar flame speed, x_{H_2} is the H_2 enrichment given by Equation (5), ϕ is the equivalence ratio and $S'_L = S'_L(x_{CO_2})$[m/s] is an intermediate flame speed (x_{CO_2} is the CO_2 content in the base biogas blend such that $x_{CO_2} = n_{CO_2}/(n_{CO_2} + n_{CH_4})$.).

3. Results and Discussion

This discussion is divided into three complementary sections. In Section 3.1, the impact of H_2 content in the S_L of biogas/air flames is discussed. Literature data on this topic were found to be scarce and, when present, focused on a narrow subset of conditions that did not support the development of a new correlation. Therefore, a numerical analysis was conducted to quantify the different effects of H_2 and CO_2 content on S_L and to provide fundamental support for the model development. Here, the results obtained from the 1D-FPF simulations are presented, and the coupling effect of CO_2 and H_2 on S_L is depicted. Section 3.2 describes the analytical model proposed in this work. The criteria used for model development are presented, and the improvement on Equations (3) and (4) is described. Furthermore, the new model's novelty is explained. Finally, the proposed correlation is validated with reliable $H_2/CO_2/CH_4$/air S_L measurements in Section 3.3.

Model predictions are compared with literature data to assess performance, and relevant cases for model application are described.

3.1. Hydrogen Content Impact on S_L

The fuel blends tested in this work are ternary mixtures of CH_4, CO_2 and H_2 in varying proportions. Each of these species impacts the laminar flame speed by changing the mixture properties: producing thermal-diffusive, kinetic and concentration effects [26,27]. Thermal-diffusive effects are caused by changes in thermal diffusivity and the specific heat capacity of the mixture. Kinetic or chemical effects occur by the participation of species in chemical reactions or pathways [28]. Concentration effects result from a reduced amount of a determined species caused by the increase of any other. Methane, carbon dioxide and hydrogen exhibit largely different properties, making their impact on any of these effects highly asymmetric. While CH_4 and H_2 are reactive species, CO_2 can be generally considered an inert gas. Regarding density, that of CO_2 is around 20 times higher than that of H_2. Thus, an understanding of these species' contributions on the effects that ultimately impact S_L is of paramount importance.

Simulations were performed for three base biogas blends: BG100 (pure CH_4), BG90 and BG80. For each of these, the range of hydrogen enrichment, as defined by Equation (5), varied within the interval $0\% \leq x_{H_2} \leq 50\%$. The equivalence ratio ϕ range was set from 0.8 to 1.0, with 0.05 steps. The obtained results are exhibited in S_L vs. x_{H_2} plots in Figures 1–3, for BG100, BG90 and BG80, respectively.

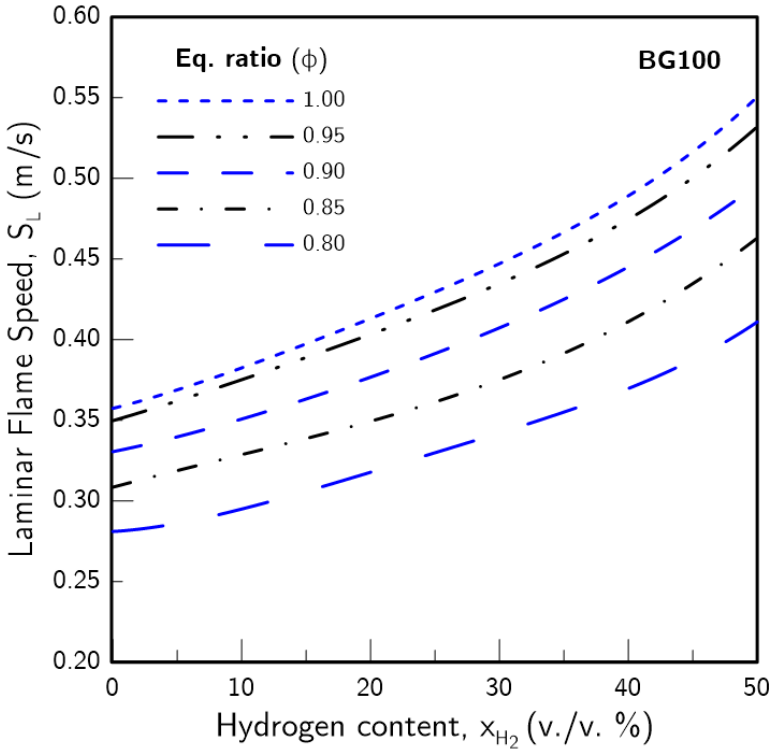

Figure 1. The laminar flame speed of biogas (BG100)/air flames enriched with H_2. Each line corresponds to the model results for a determined equivalence ratio (ϕ). Conditions were set at $p = 1$ atm and $T_u = 298$ K.

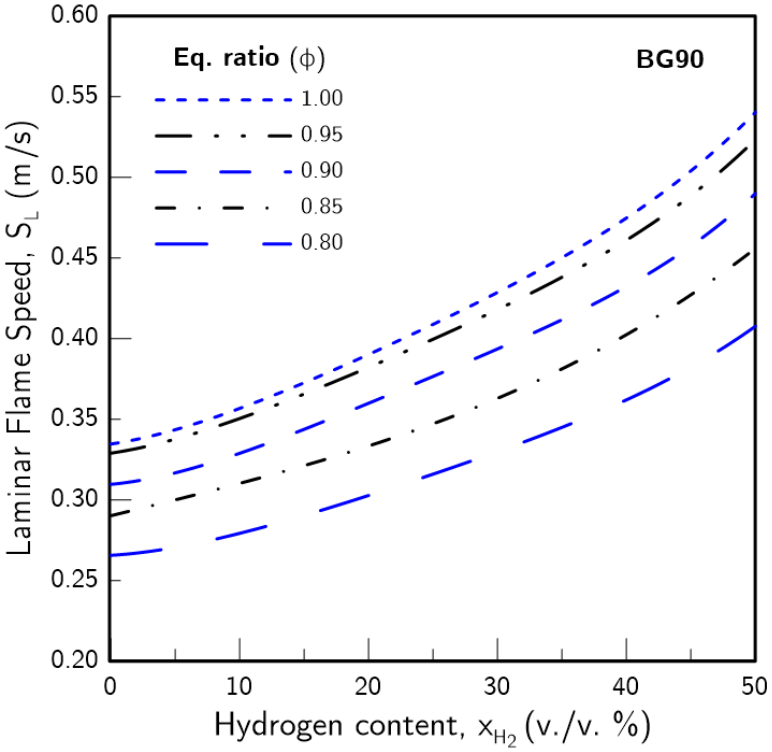

Figure 2. Laminar flame speed of BG90/air flames enriched with H_2. Each line corresponds to the model results for a determined equivalence ratio (ϕ). Conditions were set at $p = 1$ atm and $T_u = 298$ K.

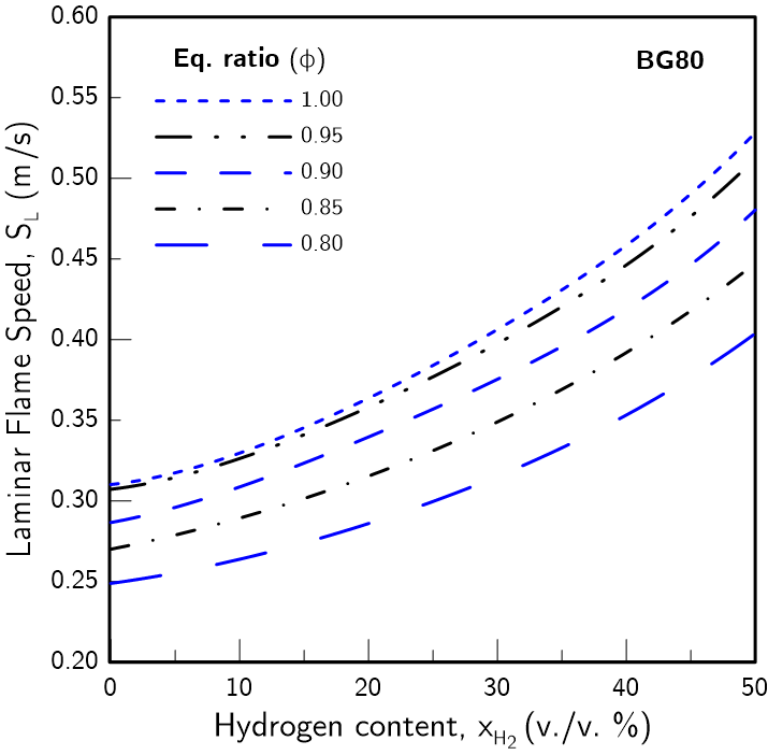

Figure 3. Laminar flame speed of BG80/air flames enriched with H_2. Each line corresponds to the model results for a determined equivalence ratio (ϕ). Conditions were set at $p = 1$ atm and $T_u = 298$ K.

Naturally, in all three cases, an increased x_{H_2} produced an increase in S_L. The thermal flame theory of Mallard and Le Chatelier [29] states that S_L is dependent on the reaction rate ($\dot{\omega}$), thermal diffusivity (α) and temperature (T (b—burned, u—unburned, i—ignition)) in the flame region in the form of Equation (7):

$$S_L = \sqrt{\alpha\dot{\omega}\left(\frac{T_b - T_i}{T_i - T_u}\right)} \quad (7)$$

Hydrogen enrichment increases α and $\dot{\omega}$, as well as temperature, thus raising S_L. A comparison of the curves exhibited in Figures 1–3 shows that hydrogen enrichment of biogas blends attenuates the negative effects of CO_2 in a non-linear fashion, with a greater proportion the higher x_{H_2} is. If an S_L average for every ϕ tested is taken at $x_{H_2} = 0\%$, it is observed that from BG100 to BG90, there is a S_L drop of 6.3%, due to the contribution of CO_2. The difference increases between BG100 and BG80, reaching 13%. However, the same calculation performed at $x_{H_2} = 50\%$ yields a drop of 1.3% from BG100 to BG90 and of 3.1% from BG100 to BG80. As a consequence, the impact of hydrogen enrichment on S_L is greater when CO_2 content is higher in the base biogas blend. On average, the S_L increase caused by $x_{H_2} = 50\%$ is of 47.3% for BG100, 58.3% for BG90 and 67.5% for BG80.

Numerical simulations conducted by Wei et al. [30] indicate that the concentration of the H radical in the flame region affects the S_L of BG/H_2 flames. Whereas H_2 increases the presence of H through the reactions R1: $OH + H_2 \longrightarrow H_2O + H$ and R2: $O + H_2 \longrightarrow H + OH$, CO_2 produces the opposite phenomena through R3: $OH + CO \longrightarrow H + CO_2$ and R4: $O + CH_3 \longrightarrow H + CH_2O$. As introduced in Section 1, R1 and R3 are the steps of the water-gas shift (WGS) sub-mechanism, which seems to be responsible for the adjustments in the H radical pool that derive from modifications in the reaction kinetics. Furthermore, CO_2 also decreases the H radical pool by diluting the mixture. Wei et al. found that the coupling effects of CO_2/H_2 for lean mixtures, as CO_2 content is increased, give rise to evident improvements of S_L through the kinetic effects of H_2. This conclusion is consistent with the results discussed above. The non-linear increase of S_L with x_{H_2}, such that $d^2S_L/dx_{H_2}^2 > 0$, supports the hypothesis that the H_2 related kinetics gradually takes over the CH_4 dominated chemical pathways. Furthermore, it seems that a larger CO_2 concentration in the base blend increases the weight of the H_2 related chemistry for lower x_{H_2}.

When considering the impact of CO_2 and H_2 on S_L, thermal-diffusive effects must also be taken into account. It is known that on top of a kinetic effect, CO_2 also produces a significant impact due to its high specific heat capacity [31]. Carbon dioxide acts as a heat sink in the flame, thus reducing the adiabatic flame temperature T_{ad} and increasing the mixture ignition temperature T_i [32,33]. In a numerical study on the impact of CO_2 dilution on CH_4/air premixed flames, Halter et al. [34] showed that for small concentrations in the flame mixture (<5%), this effect contributes to approximately 50% of the S_L reduction experienced. On the other hand, H_2 enrichment increases S_L not only through kinetics, but also as a result of thermal-diffusive effects. The increased thermal diffusivity of hydrogen produces a positive effect on S_L (see Equation (7)), counterbalancing the negative impacts of carbon dioxide. Furthermore, the lower T_i and higher T_{ad} of H_2 produce a temperature increase throughout the flame region. This effect has been reported by Rocha et al. [35] in a numerical and experimental work where the impact of H_2 on the chemiluminescence of $CH_4/CO_2/H_2$/air flames was evaluated. The simulation results of the present work (Figures 1–3) are congruent with previous research, manifesting an overall positive effect of H_2 enrichment on the S_L of biogas/air flames, even though it varies with base blend composition due to coupling CO_2/H_2 effects.

To evaluate the effects of CO_2 when combined with H_2 enrichment on S_L, further simulations were conducted. To this end, two base blends were selected: BG100 and BG80. However, to isolate the different effects of CO_2 presence, simulations were also conducted with fake CO_2 (FCO_2) in the biogas blend. This species possesses the same transport and thermodynamic properties of CO_2, but does not participate in any chemical reaction.

Thus, with ϕ set at 0.9, three S_L curves were obtained for BG100, BG80 and BG80 (FCO_2). The results are provided in Figure 4.

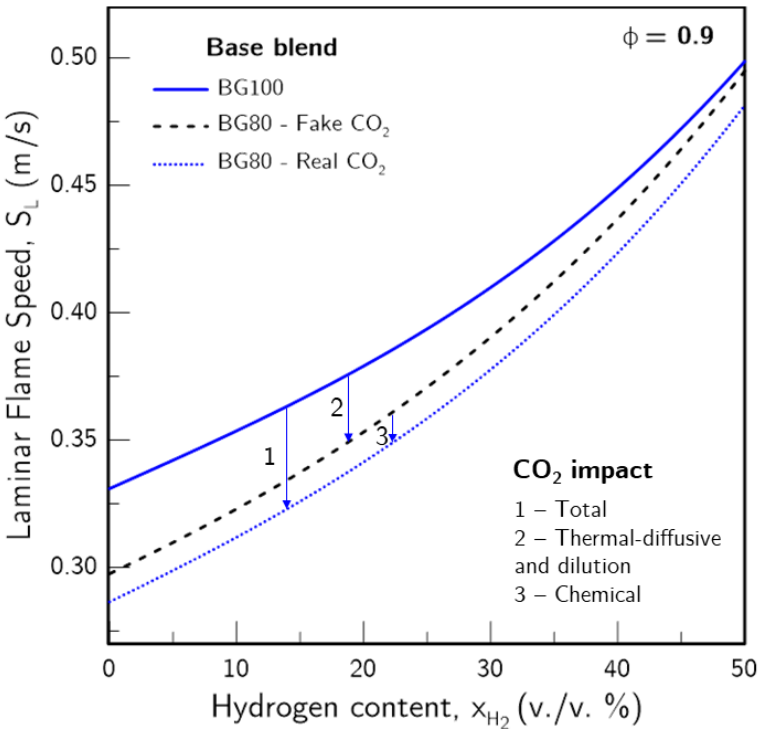

Figure 4. Laminar flame speed of BG100, BG80 and BG80 (FCO_2)/air flames enriched with H_2. Each line corresponds to the model results for a determined base blend. Conditions were set at $p = 1$ atm and $T_u = 298$ K.

The different impacts CO_2 produces in S_L for varying levels of H_2 enrichment can be seen in Figure 4. As FCO_2 does not take part in the reaction chemistry, the difference between the BG100 and BG80 (FCO_2) curves can be attributed to the dilution and thermal-diffusive effects produced by CO_2, whereas the step from BG80 (FCO_2) to BG80 stems from the CO_2 impact on the kinetics. The results show that for low H_2 content, most of the CO_2 impact on S_L can be attributed to dilution and thermal-diffusive effects. When $x_{H_2} = 0\%$, the S_L of BG80 is 0.041 m/s lower than that of BG100, with 73% of this reduction caused by thermal-diffusive and dilution effects and 27% by kinetics. However, as x_{H_2} is increased, the weight of thermal-diffusive and concentration effects is reduced. At $x_{H_2} = 50\%$, the S_L drop between the same base blends is of 0.016 m/s, with 84% of it resulting from changes in chemistry due to the presence of CO_2. Thus, whereas CO_2 thermal-diffusive and dilution effects gradually subside as H_2 content is increased, CO_2 chemistry maintains a consistent contribution in S_L reduction. The simulation results indicate that the coupling of H_2 enrichment with CO_2 in the base biogas blend tends to mitigate the negative thermal-diffusive and dilution effects on S_L caused by the latter.

As stated previously, the impact of H_2 and CO_2 on the H radical pool is linked to variations in laminar flame speed [30]. Additionally, as the dominant decomposition product of methane, the radical CH_3 is an indicator of the CH_4 related chemistry [36]. Thus, to assess in further detail the H_2 and CO_2 chemical impact on S_L, the evolution of CH_3 and H was analysed for the conditions of this study. For the same blends that produced the results exhibited in Figure 4 at $\phi = 0.9$, a CH_3 and H weight was estimated to evaluate the radical pool of both species. The contribution for each blend was computed by integrating the molar fraction of each species along the reaction distance: $\int x_{H,CH_3} dz$. This calculation is illustrated in Figure 5 through the shadowed areas. Figure 6 exhibits the evolution of the CH_3 and H radical pool with H_2 content.

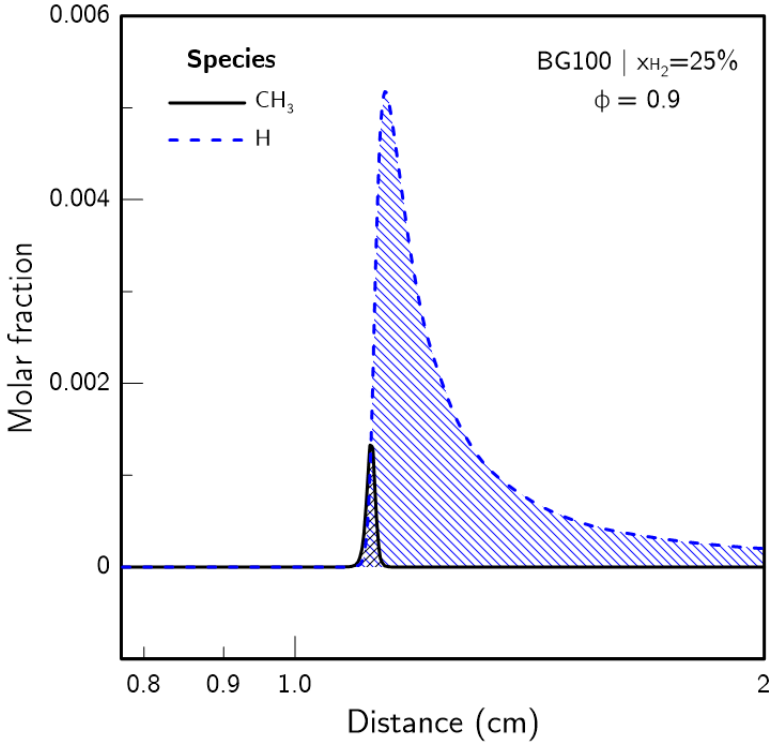

Figure 5. CH_3 and H molar fraction profile for BG100 with $x_{H_2} = 25\%$ and $\phi = 0.9$. The X axis is in the base 10 logarithmic scale. Conditions were set at $p = 1$ atm and $T_u = 298$ K.

Figure 6 shows that the CH_3 evolution with H_2 content is non-linear, such that $d^2CH_{3,w}/dx_{H_2}^2 < 0$. As CH_3 is a marker of CH_4 related chemistry, it would be expected that its weight diminishes as x_{H_2} is increased. However, the reduction of CH_3 weight is not proportional to the CH_4 concentration in the flame mixture. Even though CO_2 lowers the overall presence of CH_3, mostly through thermal-diffusive and concentration effects, it seems to have little impact on the evolution of the CH_3 radical weight with x_{H_2}. This trend indicates that as H_2 content is increased, a transition occurs, consisting of a weakening of the CH_4 related chemistry and improvement of the H_2 related kinetics. As Wei et al. [30] reported in their work, the H radical evolution appears to follow the variations in laminar flame speed through changes in the WGS sub-mechanism. However, when comparing the curves of Figures 4 and 6, it can be seen that as x_{H_2} increases, the difference between the BG100 and BG80 S_L curves reduces faster than the difference between the H radical weight. It appears that as H_2 content is increased, the CO_2 thermal-diffusive and dilution effects maintain a more relevant impact on the H radical pool than on S_L. For the BG80 base blend, a $x_{H_2} \approx 25\%$ is required to raise the H radical weight levels to those of BG100 without H_2 enrichment even though S_L is matched at $x_{H_2} \approx 17\%$. As CO_2 thermal-diffusive and dilution effects seem to produce a greater impact on H evolution than on S_L, this indicates that H_2 not only increases S_L through a more efficient H radical production, but also due to its own thermal-diffusive and concentration effects.

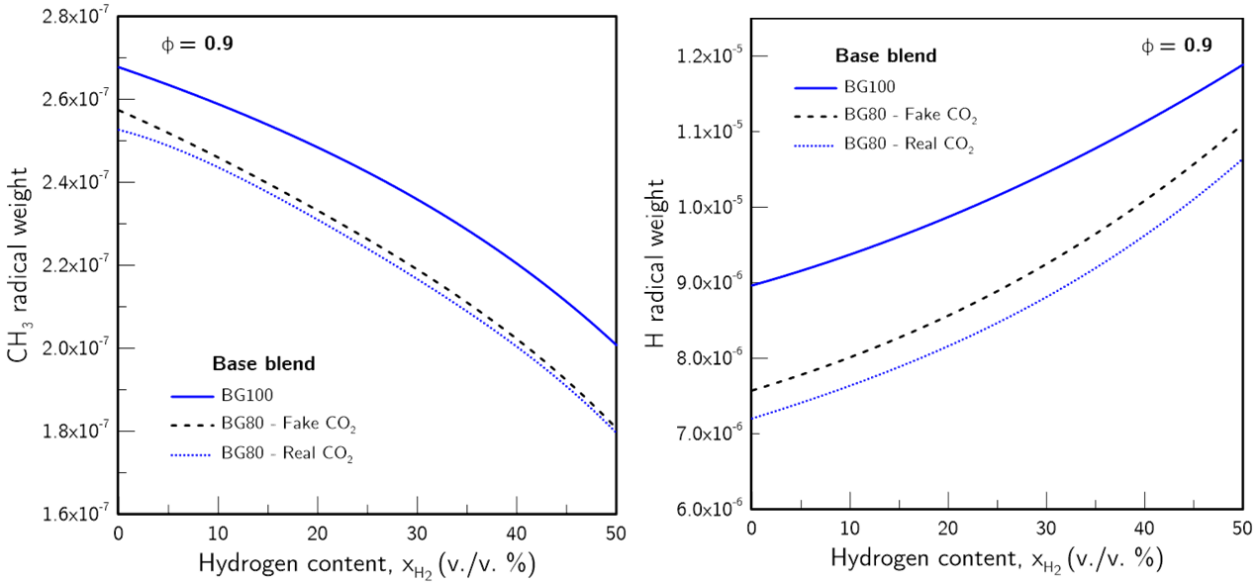

Figure 6. CH_3 and H weight BG100, BG80 and BG80 (FCO_2)/air flames with varying x_{H_2}. The equivalence ratio is 0.9. Conditions were set at $p = 1$ atm and $T_u = 298$ K.

The above-mentioned effect of CO_2 and H_2 on S_L turns the modelling of their impact into a complex task. In the next section, the steps taken to obtain a simple analytical model to quantify the impact of H_2 enrichment on the S_L of lean biogas/air flames are described.

3.2. Analytical Model

As stated in Section 1, this work aims to develop a correlation to model the impact of H_2 enrichment (up to 50%) on the S_L of lean biogas/air flames. Currently, available correlations are either too complex to allow an expeditious use or are not tailored to hydrogen-enriched biogas blends [19,37]. Because of this, existing expressions require a priori undertakings to determine several fit parameters or to adapt mathematical formulations. Their complexity requires, in some cases, the estimation of several fit parameters on a case-by-case basis, hindering the expeditious aim of a correlation of this sort. Hence, it seems that these alternatives only seem applicable in an academic or advanced industry environment where computational cost might not be a significant issue. Additionally, these alternatives fail to specifically address the case of H_2-enriched biogas, thus combining the contributions of hydrogen and carbon dioxide in fit parameters that also depend on other variables. This implies that the user of any of these models has to determine new fit parameters every time the base biogas blend or the hydrogen enrichment level are changed, as x_{H_2} and x_{CO_2} are not function arguments. Here, simplicity and fast use were adopted as priorities to improve on the options already available in the literature.

In a previous work, Quintino and Fernandes [20] quantified the impact of CO_2 dilution on the S_L of CH_4/air lean flames and introduced a new analytical model to predict this effect. The final model is presented in Equation (4), and its details can be found in the original research. Thus, for the new model, it was intended to achieve an expression that isolated in different terms the contributions of CO_2 and H_2 for the S_L of $CH_4/CO_2/H_2$/air lean flames. To this end, Equation (4) was adopted to estimate an intermediate flame speed $S'_L(x_{CO_2})$ that encompasses the effect of CO_2 in the base biogas blend. Based on the simulation outputs presented in the previous section, an iterative procedure as described in Section 2 was employed to obtain the model. Considering the curves in Figures 1–3, the following constraints were set: $dS_L/dx_{H_2} > 0$ and $d^2S_L/dx_{H_2}^2 > 0$ for $0\% \leq x_{H_2} \leq 50\%$. Furthermore, a minimum coefficient of determination $\left(R^2\right)$ of 0.99 was ensured. For the formulations tested that complied with all established criteria, the choice was based on the expression's simplicity.

Based on this approach, the following correlation for the impact of H_2 enrichment on the S_L of biogas/air lean flames is proposed:

$$S_L(x_{H_2}) = \frac{\zeta(\phi)}{S'_L(x_{CO_2})} x_{H_2} e^{x_{H_2}} + S'_L(x_{CO_2}) \quad (8)$$

where $S_L = S_L(x_{H_2})$ is the laminar flame speed of the H_2-enriched flame mixture, $S'_L = S'_L(x_{CO_2})$ is the intermediate flame speed computed with Equation (4), x_{CO_2} is the CO_2 content of the base biogas blend, x_{H_2} is the hydrogen fraction in the flame mixture (Equation (5)) and $\zeta = \zeta(\phi)$ is a fit parameter that varies with the equivalence ratio ϕ. The variation of ζ with ϕ was evaluated, and a data fit was performed. The values obtained and the correspondent data fit can be found in Figure 7. The obtained expression took the form: $\zeta(\phi) = -0.3143 \times \phi^2 + 0.7437 \times \phi - 0.35$, with $R^2 = 0.9974$.

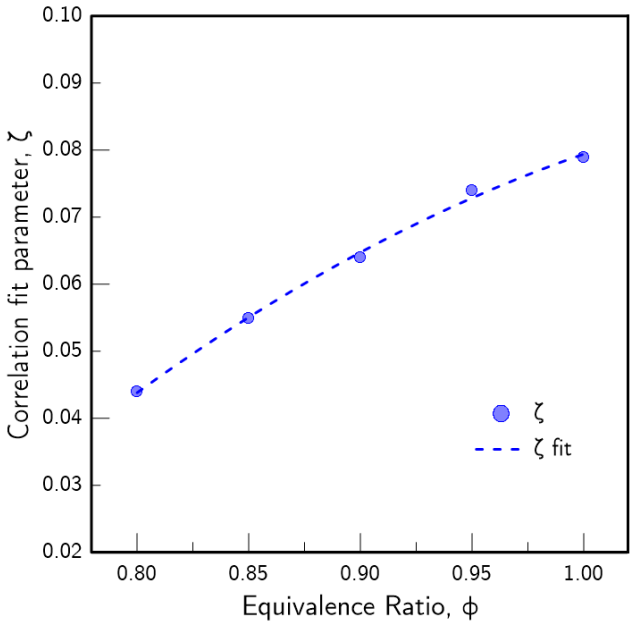

Figure 7. Variation of the fit parameter ζ with the equivalence ratio. The correspondent data fit curve is also displayed.

The final model compared well with the numerical results. The lowest coefficient of determination ($R^2 = 0.9903$) was found for BG80 at $\phi = 1.0$ and the highest ($R^2 = 0.9983$) for BG100 at $\phi = 1.0$.

The model proposed by Quintino and Fernandes [20] in 2018 improved the original correlation established by Metgalchi and Keck [14] in 1982 by re-defining fit parameters and modifying the term that quantifies the impact of diluents in the mixture. Equation (4) models the effect of CO_2 concentration on the laminar flame speed of biogas/air flames, which permits a fast estimation of S_L for varying biogas composition. Equation (4) proved to be a significant improvement on Equation (3), which was shown to fail for biogas blends [20]. Thus, Equation (4) extended the original range of application of Equation (3) by accurately predicting the impact of CO_2 content on S_L. However, this improved correlation did not account for the possibility of blending other fuels with biogas. The model proposed in Equation (8) predicts the S_L of biogas when enriched with H_2, thus extending the range of application of Equations (3) and (4). The most significant novelty of this work is that the developed model (Equation (8)) only requires a single fit parameter $\zeta(\phi)$ for the S_L prediction of H_2-enriched biogas/air flames. In opposition to alternative correlations, where lookup tables are required to readjust parameters according to blend composition, the new model proposed in this work is ready to use for CO_2 content up to 20% in the biogas blend and H_2 enrichment up to 50%.

3.3. Validation

As stated above, the analytical model of Equation (8) presented values in agreement with the numerical simulations performed. To validate the developed model, a collection of results from the literature was compared to the model predictions. These publications encompassed different numerical and experimental methods of S_L determination, as well as base blends with two levels of CO_2 content (BG100 and BG80). This collection is compiled and summarized in Table 2.

Table 2. Published work on laminar flame speed of lean $CH_4/CO_2/H_2$/air flames used to validate the correlation of this work.

Authors	Method	ϕ	p	T_u	Ref.
Hermanns	Heat flux burner	0.8, 0.9, 1.0	1 atm	298 K	[38]
Coppens et al.	Heat flux burner	0.8, 0.9, 1.0	1 atm	298 K	[37]
Halter et al.	Constant volume bomb	0.8, 0.9, 1.0	1 bar	298 K	[39]
Yadav et al.	Flat flame burner and Ansys (GRI3.0)	0.8, 0.9, 1.0	1 bar	298 K	[40]
Wei et al.	Premix Code (GRI3.0)	0.9, 1.0	1 atm	298 K	[30]

The first two references of Table 2 employ the heat flux burner method to estimate S_L [37,38]. A constant volume bomb experiment is also included [39], as well as tests with a flat flame burner [40]. Simulations ran with Ansys [40] and Premix Code [30] fed with the GRI-Mech 3.0 mechanism [41] were also used.

Based on the developed model (Equation (8)) and on available literature results, two data sets are plotted, for BG100 and BG80. For each base blend, literature data are plotted against model predictions in the range $0\% \leq x_{H_2} \leq 50\%$ and for $\phi = 0.8, 0.9, 1.0$. The resulting graphs are exhibited in Figures 8 and 9, for BG100 and BG80, respectively.

Overall, the correlation predictions exhibited good concordance with the literature data. The agreement was better at $\phi = 0.9$ and 1.0, with similar performance whether the base blend was BG100 or BG80. A detailed evaluation of the data in both plots shows that the average percentage difference between the correlation prediction and literature data was 4.44% for BG100 (Figure 8) and 4.02% for BG80 (Figure 9). For the case of BG100, differences lied within the interval $[0.09, 15.62]\%$, whereas for BG80 this interval was $[0.09, 12.02]\%$. The highest differences were found for $\phi = 0.8$, where the correlation tended to overestimate the literature data, even though the difference never exceeded 0.056 m/s. The highest differences were found in the data of Figure 8, where the correlation prediction was considerably higher than the data collected from the work developed by Halter et al. [39]. In their work, a spherical combustion chamber was coupled to a shadowgraphy system, and flame pictures were captured by a high-speed camera. Experiments were conducted for CH_4/H_2/air flames with the global equivalence ratio varying from 0.7 to 1.2. These were then compared to CHEMKIN simulations fed with the GRI-Mech 3.0 kinetics mechanism [41]. Measurements performed by Halter et al. (Figure 7 of reference [39]) at $\phi = 0.8$ exhibited the poorest agreement with CHEMKIN simulations and seemed to contrast with other published data. Thus, it appears that the impact of H_2 content on S_L was well captured by the model of the present work. The literature data also exhibited a non-linear S_L increase with x_{H_2}. This supports the hypothesis, stated in Section 3.1, that the H_2 related kinetics takes over the CH_4 related one as x_{H_2} is increased.

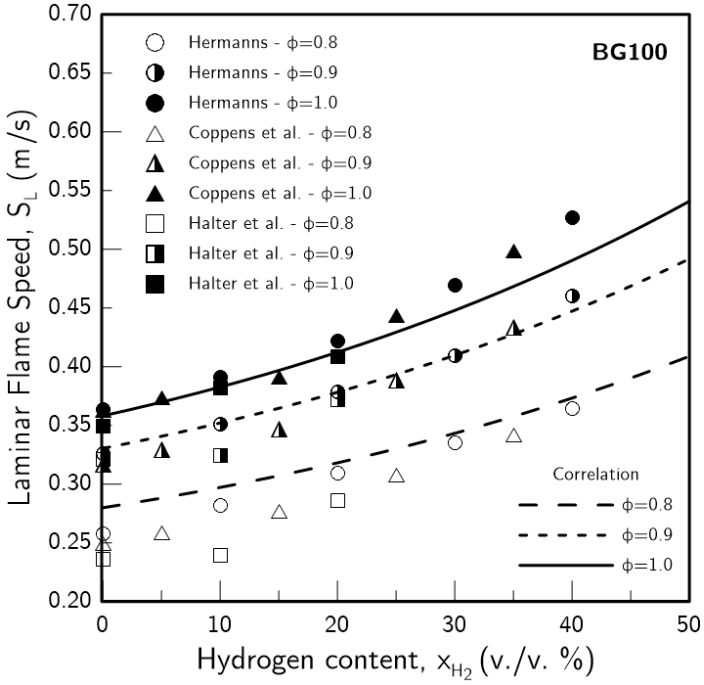

Figure 8. Laminar flame speed of H_2-enriched BG100/air flames. Symbols are literature results, and lines are the application of the correlation of this work.

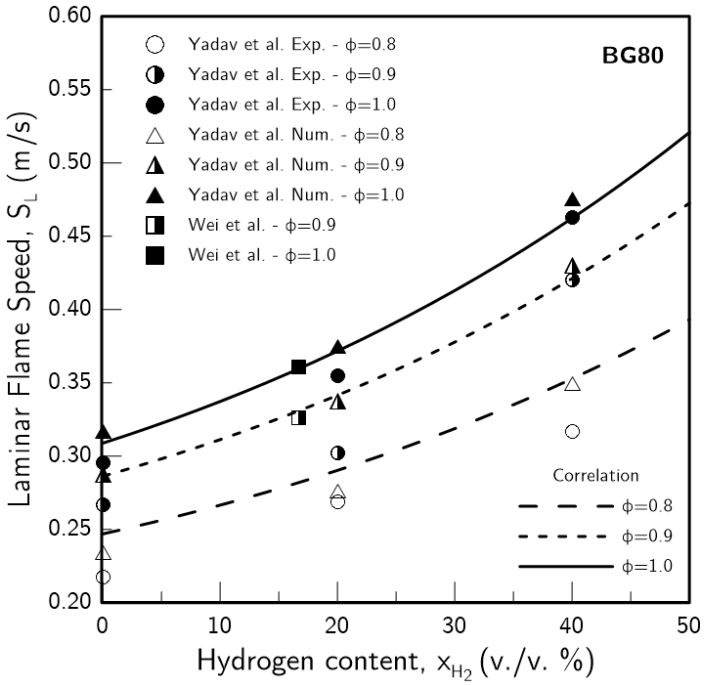

Figure 9. Laminar flame speed of H_2-enriched BG80/air flames. Symbols are the literature results, and lines are the application of the correlation of this work.

On top of the comparison with the literature data, model predictions were evaluated with every S_L value resulting from the performed simulations. Numerical results were compared to model predictions to evaluate if any subset of points were poorly captured by the developed correlation. Figure 10 exhibits this analysis' output.

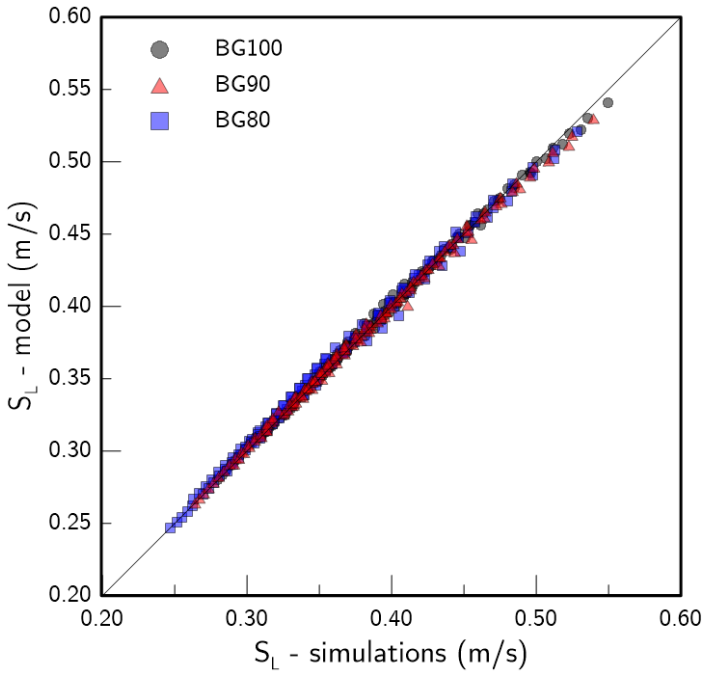

Figure 10. Model predictions vs. the numerical results of laminar flame speed S_L. Symbols indicate base biogas compositions. All equivalence ratio and H_2 enrichment conditions produced in this work are included.

The data in Figure 10 demonstrate that the correlation displayed a good performance not only on average, but also for the complete set of numerical data produced in this work. There were no significant accuracy differences identified among BG100, BG90 and BG80. The percentage difference between the correlation predictions and simulations never exceeded 2.91%, with an average difference of 0.74%. Thus, the model in Equation (8) can be considered an accurate representation of the S_L values yielded by the simulations conducted in Cantera with USC-Mech 2.0. Overall, the analytical model exhibited a good agreement with the experiments, indicating that numerical simulations also compared well with the literature data.

This new model should be particularly relevant in burner design and gas interchangeability analysis involving $CH_4/CO_2/H_2$ blends. Examples of this are the research developed by Jones et al. [42] and Vries et al. [43], where flashback and blowoff limits for domestic appliances were evaluated in a context where hydrogen is blended in the fuel feed. The determination of the theoretical flame stability first requires a prediction of the flame speed as a function of hydrogen content. The model developed in this work is tailored for these sorts of analysis, given its low average uncertainty of 0.74% when compared with simulations and 4.44% when compared with literature data. Therefore, it provides an accurate description of S_L for CO_2 content up to 20% in the biogas blend and H_2 enrichment up to 50%.

4. Conclusions

In this work, 1D FPF simulations were conducted in Cantera to assess the impact of H_2 enrichment on the S_L of biogas/air lean flames. Furthermore, numerical results were employed in the development of an analytical correlation to model this effect. Simulations were conducted for three base biogas blends (BG100, BG90 and BG80) with H_2 content in the fuel mixture (x_{H_2}) up to 50% and an equivalence ratio (ϕ) between 0.8 and 1.0. The approach undertaken in this work allowed the quantification of CO_2 and H_2 effects on S_L, by evaluating the dilution, thermal-diffusive and chemical impacts. The numerical model made it possible to run simulations with both real (CO_2) and fake (FCO_2) carbon

dioxide to isolate the different effects of its presence on S_L. Finally, the analytical correlation was tested against data from the literature. The main findings are summarized below:

1. The introduction of H_2 in the fuel blends produced a greater effect on S_L the higher the CO_2 content was. Furthermore, the increase in S_L due to H_2 enrichment was non-linear, with a more pronounced effect the higher x_{H_2} was. This was found to be linked with an increase in the H radical pool, which resulted from greater H production through the sub-mechanism of the water-gas shift (WGS) reaction.
2. The presence of H_2 in the fuel blend tended to mitigate the thermal-diffusive and concentration effects of CO_2 on S_L. These effects were the highest contributor for S_L reduction for low x_{H_2}. However, these gradually subsided as x_{H_2} increased, while the CO_2 chemistry maintained a consistent impact. Thus, for practical applications, higher amounts of H_2-enrichment may avoid the need to completely remove carbon dioxide from biogas blends.
3. H_2 enrichment was found to weaken the CH_4 related chemistry as the CH_3 radical pool was significantly impacted. The reduction of the CH_3 radical presence was found to be not directly proportional to the CH_4 concentration, with an acceleration of its reduction with increasing x_{H_2}.
4. Based on the numerical results, a new correlation to model the impact of H_2 enrichment on the S_L of lean biogas/air flames was proposed:

$$S_L(x_{H_2}) = \frac{\zeta(\phi)}{S'_L(x_{CO_2})} x_{H_2} e^{x_{H_2}} + S'_L(x_{CO_2}) \quad (9)$$

where $S_L = S_L(x_{H_2})$ is the laminar flame speed of the H_2-enriched flame mixture, $S'_L = S'_L(x_{CO_2})$ is the intermediate flame speed computed with Equation (4), x_{CO_2} is the CO_2 content of the base biogas blend, x_{H_2} is the hydrogen fraction in the flame mixture (Equation (5)) and $\zeta = \zeta(\phi)$ is a fit parameter. The correlation exhibited good agreement with literature data and with simulations for all of the tested conditions. This new model isolates the contribution of H_2 and CO_2 as both are arguments of the function that yield $S_L = S_L(x_{H_2}, \phi, S'_L(x_{CO_2}))$. Thus, the final model can be directly used to estimate S_L without the need for a priori adaptations of fit parameters for varying base blends as the correlation itself accomplishes that goal. The fast and reliable estimation of S_L for H_2-enriched biogas blends makes this model useful for the adaptation or development of existing devices that rely on these blends.

Concluding remarks:

The model proposed in this work provides an engineering approach to estimate S_L for fuel-lean combustion of H_2-enriched biogas blends. In contexts where biogas is widely available, the admixture of renewable hydrogen can improve equipment performance or even allow the possibility of using lower quality biogas blends, which would otherwise remain unused or burned in flares. Future research could address fuel-rich conditions. These configurations, typically found in the ceramics and glass industry for radiative heat transmission purposes, will eventually shift from natural gas to renewable gases. The use of biogas will likely require hydrogen admixture to compensate for the loss in CH_4. The development of an analytical model for fuel-rich conditions will require a reassessment of reaction kinetics and an adaptation of the original model proposed by Quintino and Fernandes in 2018 [20]. The USC Mech 2.0, employed in this research, should cope well with such conditions since it was subject to validation with proven H_2/CO/C_1-C_4 combustion data. However, the development of a new correlation for fuel-rich conditions must cope with the variability of the maxima location in relation to the equivalence ratio. The hydrogen enrichment of biogas, in fuel-rich conditions, will push the maximum value of S_L for higher values of ϕ as x_{H_2} is increased. This phenomena must be well captured by any new model proposed in the future.

Author Contributions: Conceptualization, F.M.Q. and E.C.F.; methodology, F.M.Q.; software, F.M.Q.; validation, F.M.Q. and E.C.F.; formal analysis, F.M.Q.; investigation, F.M.Q.; resources, E.C.F.; data curation, F.M.Q.; visualization, F.M.Q.; writing, original draft preparation, F.M.Q.; writing, review and editing, E.C.F.; supervision, E.C.F. All authors read and agreed to the published version of the manuscript.

Funding: F.M. Quintino acknowledges Fundação para a Ciência e Tecnologia for the provision of the scholarship PD/BD/140184/2018.

Conflicts of Interest: The authors declare no conflict of interest.

Abbreviations

The following abbreviations are used in this manuscript:

1D	One-dimensional
BG	Biogas
EGR	Exhaust gas recirculation
FPF	Freely propagating flame
USC	University of Southern California
WGS	Water-gas shift

References

1. Gillingham, K.; Huang, P. Is abundant natural gas a bridge to a low-carbon future or a dead-end? *Energy J.* **2019**, *40*. [CrossRef]
2. Speirs, J.; Balcombe, P.; Johnson, E.; Martin, J.; Brandon, N.; Hawkes, A. A greener gas grid: What are the options. *Energy Policy* **2018**, *118*, 291–297. [CrossRef]
3. Glenk, G.; Reichelstein, S. Economics of converting renewable power to hydrogen. *Nat. Energy* **2019**, *4*, 216–222. [CrossRef]
4. Lantz, M. *Biogas in Sweden-Opportunities and Challenges from a Systems Perspective*; Lund University: Lund, Sweden, 2013.
5. Patricio, R.; Sales, A.; Sacramento, E.; De Lima, L.; Veziroglu, T. Wind hydrogen energy system and the gradual replacement of natural gas in the State of Ceará–Brazil. *Int. J. Hydrogen Energy* **2012**, *37*, 7355–7364. [CrossRef]
6. Roubík, H.; Mazancová, J.; Le Dinh, P.; Dinh Van, D.; Banout, J. Biogas quality across small-scale biogas plants: A case of central Vietnam. *Energies* **2018**, *11*, 1794. [CrossRef]
7. Korberg, A.D.; Skov, I.R.; Mathiesen, B.V. The role of biogas and biogas-derived fuels in a 100% renewable energy system in Denmark. *Energy* **2020**, *199*, 117426. [CrossRef]
8. Saccani, C.; Pellegrini, M.; Guzzini, A. Analysis of the Existing Barriers for the Market Development of Power to Hydrogen (P2H) in Italy. *Energies* **2020**, *13*, 4835. [CrossRef]
9. Quintino, F.M.; Fernandes, E.C. Interchangeability Analysis of Biogas and Hydrogen Blends. In Proceedings of the 27th European Biomass Conference and Exhibition Proceedings, Lisbon, Portugal, 27–30 May 2019; pp. 736–741. [CrossRef]
10. Barlow, R.; Frank, J.; Karpetis, A.; Chen, J.Y. Piloted methane/air jet flames: Transport effects and aspects of scalar structure. *Combust. Flame* **2005**, *143*, 433–449. [CrossRef]
11. Turns, S.R. *Introduction to Combustion*; McGraw-Hill Companies: New York, NY, USA, 1996; Volume 287.
12. Lu, T.; Law, C.K. Toward accommodating realistic fuel chemistry in large-scale computations. *Prog. Energy Combust. Sci.* **2009**, *35*, 192–215. [CrossRef]
13. Lu, T.; Law, C.K. A directed relation graph method for mechanism reduction. *Proc. Combust. Inst.* **2005**, *30*, 1333–1341. [CrossRef]
14. Metghalchi, M.; Keck, J.C. Burning velocities of mixtures of air with methanol, isooctane, and indolene at high pressure and temperature. *Combust. Flame* **1982**, *48*, 191–210. [CrossRef]
15. Gülder, O. Burning velocities of ethanol–air and ethanol–water–air mixtures. *AIAA Progr Astronaut Aeronaut* **1984**, *95*, 181–197.
16. Liao, S.; Jiang, D.; Cheng, Q. Determination of laminar burning velocities for natural gas. *Fuel* **2004**, *83*, 1247–1250. [CrossRef]
17. Han, P.; Checkel, M.D.; Fleck, B.A.; Nowicki, N.L. Burning velocity of methane/diluent mixture with reformer gas addition. *Fuel* **2007**, *86*, 585–596. [CrossRef]
18. Elia, M.; Ulinski, M.; Metghalchi, M. Laminar burning velocity of methane–air–diluent mixtures. *J. Eng. Gas Turbines Power* **2001**, *123*, 190–196. [CrossRef]
19. Bougrine, S.; Richard, S.; Nicolle, A.; Veynante, D. Numerical study of laminar flame properties of diluted methane-hydrogen-air flames at high pressure and temperature using detailed chemistry. *Int. J. Hydrogen Energy* **2011**, *36*, 12035–12047. [CrossRef]
20. Quintino, F.; Fernandes, E. Analytical correlation to model diluent concentration repercussions on the burning velocity of biogas lean flames: Effect of CO_2 and N_2. *Biomass Bioenergy* **2018**, *119*, 354–363. [CrossRef]
21. Goodwin, D.G.; Moffat, H.K.; Speth, R.L. *Cantera: An Object-Oriented Software Toolkit for Chemical Kinetics, Thermodynamics, and Transport Processes*; Caltech: Pasadena, CA, USA, 2009.
22. Wang, H.; You, X.; Joshi, A.V.; Davis, S.G.; Laskin, A.; Egolfopoulos, F.; Law, C.K.; Version II, U.M. High-Temperature Combustion Reaction Model of H_2. Technical Report; CO/C1–C4 Compounds. 2007. Available online: http://ignis.usc.edu/Mechanisms/USC-MechII/USC_MechII.htm (accessed on 14 December 2020).

23. Zhang, Y.; Jiang, X.; Wei, L.; Zhang, J.; Tang, C.; Huang, Z. Experimental and modeling study on auto-ignition characteristics of methane/hydrogen blends under engine relevant pressure. *Int. J. Hydrogen Energy* **2012**, *37*, 19168–19176. [CrossRef]
24. Ren, F.; Chu, H.; Xiang, L.; Han, W.; Gu, M. Effect of hydrogen addition on the laminar premixed combustion characteristics the main components of natural gas. *J. Energy Inst.* **2019**, *92*, 1178–1190. [CrossRef]
25. Qian, Y.; Sun, S.; Ju, D.; Shan, X.; Lu, X. Review of the state-of-the-art of biogas combustion mechanisms and applications in internal combustion engines. *Renew. Sustain. Energy Rev.* **2017**, *69*, 50–58. [CrossRef]
26. Xie, Y.; Wang, J.; Xu, N.; Yu, S.; Huang, Z. Comparative study on the effect of CO_2 and H_2O dilution on laminar burning characteristics of CO/H_2/air mixtures. *Int. J. Hydrogen Energy* **2014**, *39*, 3450–3458. [CrossRef]
27. Chen, Z.; Tang, C.; Fu, J.; Jiang, X.; Li, Q.; Wei, L.; Huang, Z. Experimental and numerical investigation on diluted DME flames: Thermal and chemical kinetic effects on laminar flame speeds. *Fuel* **2012**, *102*, 567–573. [CrossRef]
28. Stylianidis, N.; Azimov, U.; Birkett, M. Investigation of the effect of hydrogen and methane on combustion of multicomponent syngas mixtures using a constructed reduced chemical kinetics mechanism. *Energies* **2019**, *12*, 2442. [CrossRef]
29. Law, C.K. *Combustion Physics*; Cambridge University Press: Cambridge, UK, 2010.
30. Wei, Z.; He, Z.; Zhen, H.; Zhang, X.; Chen, Z.; Huang, Z. Kinetic modeling investigation on the coupling effects of H_2 and CO_2 addition on the laminar flame speed of hydrogen enriched biogas mixture. *Int. J. Hydrogen Energy* **2020**, *45*, 27891–27903. [CrossRef]
31. Glarborg, P.; Bentzen, L.L. Chemical effects of a high CO_2 concentration in oxy-fuel combustion of methane. *Energy Fuels* **2008**, *22*, 291–296. [CrossRef]
32. Xie, Y.; Wang, J.; Zhang, M.; Gong, J.; Jin, W.; Huang, Z. Experimental and numerical study on laminar flame characteristics of methane oxy-fuel mixtures highly diluted with CO_2. *Energy Fuels* **2013**, *27*, 6231–6237. [CrossRef]
33. Westbrook, C.K.; Dryer, F.L. Chemical kinetic modeling of hydrocarbon combustion. *Prog. Energy Combust. Sci.* **1984**, *10*, 1–57. [CrossRef]
34. Halter, F.; Foucher, F.; Landry, L.; Mounaïm-Rousselle, C. Effect of dilution by nitrogen and/or carbon dioxide on methane and iso-octane air flames. *Combust. Sci. Technol.* **2009**, *181*, 813–827. [CrossRef]
35. Rocha, N.; Quintino, F.; Fernandes, E. H_2 enrichment impact on the chemiluminescence of biogas/air premixed flames. *Int. J. Hydrogen Energy* **2020**, *45*, 3233–3250. [CrossRef]
36. Zhang, X.; Mei, B.; Ma, S.; Pan, H.; Wang, H.; Li, Y. Experimental and kinetic modeling investigation on laminar flame propagation of CH_4/CO mixtures at various pressures: Insight into the transition from CH4 related chemistry to CO related chemistry. *Combust. Flame* **2019**, *209*, 481–492. [CrossRef]
37. Coppens, F.; De Ruyck, J.; Konnov, A.A. Effects of hydrogen enrichment on adiabatic burning velocity and NO formation in methane+ air flames. *Exp. Therm. Fluid Sci.* **2007**, *31*, 437–444. [CrossRef]
38. Hermanns, R.T.E. Laminar Burning Velocities of Methane-Hydrogen-Air Mixtures. Ph.D. Thesis, Technische Universiteit Eindhoven, Eindhoven, The Netherlands, 2007.
39. Halter, F.; Chauveau, C.; Djebaïli-Chaumeix, N.; Gökalp, I. Characterization of the effects of pressure and hydrogen concentration on laminar burning velocities of methane–hydrogen–air mixtures. *Proc. Combust. Inst.* **2005**, *30*, 201–208. [CrossRef]
40. Yadav, V.K.; Ray, A.; Ravi, M. Experimental and computational investigation of the laminar burning velocity of hydrogen-enriched biogas. *Fuel* **2019**, *235*, 810–821. [CrossRef]
41. Smith, G.P.; Golden, D.M.; Frenklach, M.; Moriarty, N.W.; Eiteneer, B.; Goldenberg, M.; Bowman, C.T.; Hanson, R.K.; Song, S.; Gardiner, W., Jr.; et al. GRI-Mech 3.0, 1999. 2011. Available online: http://www.me.berkeley.edu/gri_mech (accessed on 14 December 2020).
42. Jones, D.R.; Al-Masry, W.A.; Dunnill, C.W. Hydrogen-enriched natural gas as a domestic fuel: An analysis based on flash-back and blow-off limits for domestic natural gas appliances within the UK. *Sustain. Energy Fuels* **2018**, *2*, 710–723. [CrossRef]
43. De Vries, H.; Mokhov, A.V.; Levinsky, H.B. The impact of natural gas/hydrogen mixtures on the performance of end-use equipment: Interchangeability analysis for domestic appliances. *Appl. Energy* **2017**, *208*, 1007–1019. [CrossRef]